

Phase Equilibria of the $\text{SiO}_2\text{-V}_2\text{O}_5$ system

Desheng Feng^a, Jianbo Zhang^b, Ming Li^b, Mao Chen^{a,*}, Baojun Zhao^a

^a School of Chemical Engineering, The University of Queensland, St Lucia, QLD, 4072, Australia

^b Pangang Group Panzhihua Steel Research Institute Co., Ltd., Panzhihua, Sichuan, 617000, China



ARTICLE INFO

Keywords:

$\text{SiO}_2\text{-V}_2\text{O}_5$ system

Phase equilibrium

EPMA

Eutectic

ABSTRACT

The $\text{SiO}_2\text{-V}_2\text{O}_5$ system is one of the key systems for vanadium extraction and applications of vanadium oxides in the ceramic industries. However, only limited data in this system and contradictive results were reported from preceding studies. In the present study, high-temperature phase equilibrium experiments were conducted to construct the phase diagram of $\text{SiO}_2\text{-V}_2\text{O}_5$ system at temperature range of 660–1100 °C. Electron probe X-ray micro-analyzer (EPMA) was used to analyze the microstructure and composition of the phases presented in quenched samples. The liquidus temperatures in both SiO_2 and V_2O_5 primary phase field were determined. The eutectic temperature is confirmed to be within 670–680 °C and the eutectic composition comprises 1.9 wt% SiO_2 . SiO_2 phase contains up to 1.4 wt% V_2O_5 in the temperature range investigated.

1. Introduction

Vanadium is an important element and attracts more and more attentions due to its vital properties. Vanadium-containing alloys have been extensively used in steels [1,2] and titanium alloys [3,4] to improve their performances. Vanadium exhibits multiple oxidation states depending on oxygen partial pressure and temperature. Vanadium can act as V(II), V(III), V(IV) and V(V) [5,6], and V_2O_5 is the most stable vanadium oxide in the temperature range between 500 to 1100 °C and P (O_2) between 1 to 10^{-2} atm [7]. The vanadium redox battery, utilizing vanadium ions in different oxidation states, has been commercialized and used as the energy storage [8]. Vanadium compounds are also used as catalysts and the most common one is V_2O_5 [9]. V_2O_5 can be supported by SiO_2 or form a homogeneous gel with SiO_2 in these catalysts to enhance the performance [10,11]. Besides, $\text{SiO}_2\text{-V}_2\text{O}_5$ melt can synthesize nanocomposites, which can be used as optical sensors [12] and structured electrodes [13]. V_2O_5 is also a colorant in ceramic and glass industries [14]. Moreover, the $\text{SiO}_2\text{-V}_2\text{O}_5$ system is one of the most fundamental systems in the vanadium extraction process for various sources such as stone coal and iron slag [15,16]. However, the phase diagram of this binary system is not well established.

Literature review shows that only two studies were carried out for the $\text{SiO}_2\text{-V}_2\text{O}_5$ system in air [17,18]. Both studies agreed that V_2O_5 and SiO_2 did not form any binary compound and no information on the solid solutions was reported [17,18]. However, they reported different liquidus temperatures, eutectic temperatures and compositions [17,18]. In Gravette et al.'s study [17], the phase diagram was determined by

measuring weight losses of SiO_2 rods in V_2O_5 melt at different temperature. Differential thermal analysis (DTA) technique was also applied to further investigate the eutectic temperature and composition. Gravette et al. determined the eutectic point with 1.1 wt% SiO_2 in liquid at 661 °C. Wang et al. [18] conducted high-temperature experiments in air, while all the samples were held in MgO crucibles and analyzed by XRD. Differential scanning calorimetry (DSC) was also adopted by these researchers [18] to determine the phase changes. Possible MgO contamination was not mentioned in their study [18], and the eutectic point was determined to be with 32 wt% SiO_2 at 570 °C. Due to the limited thermodynamic data, FactSage thermodynamic software [19] could not calculate the phase diagram containing V_2O_5 .

Large discrepancies in the reported $\text{SiO}_2\text{-V}_2\text{O}_5$ phase diagrams [17,18] indicate the experimental difficulties, as V_2O_5 may volatilize quickly above its melting point [20]. Advanced high-temperature experimental techniques and post-experimental compositional analysis were applied to determine the $\text{SiO}_2\text{-V}_2\text{O}_5$ phase diagram at temperature range of 660–1100 °C.

2. Experimental methodology

High-temperature equilibrium experiments were conducted in air to investigate the $\text{SiO}_2\text{-V}_2\text{O}_5$ system. Briefly, the sample was held at high temperatures to allow the solid-liquid reactions to reach equilibrium. After equilibration, the sample was quenched so the phase assemblages at high temperatures could be retained and the liquid phase was

* Corresponding author.

E-mail address: mao.chen@uq.edu.au (M. Chen).

<https://doi.org/10.1016/j.ceramint.2020.06.183>

Received 29 April 2020; Received in revised form 10 June 2020; Accepted 16 June 2020

Available online 24 June 2020

0272-8842/ © 2020 Elsevier Ltd and Techna Group S.r.l. All rights reserved.

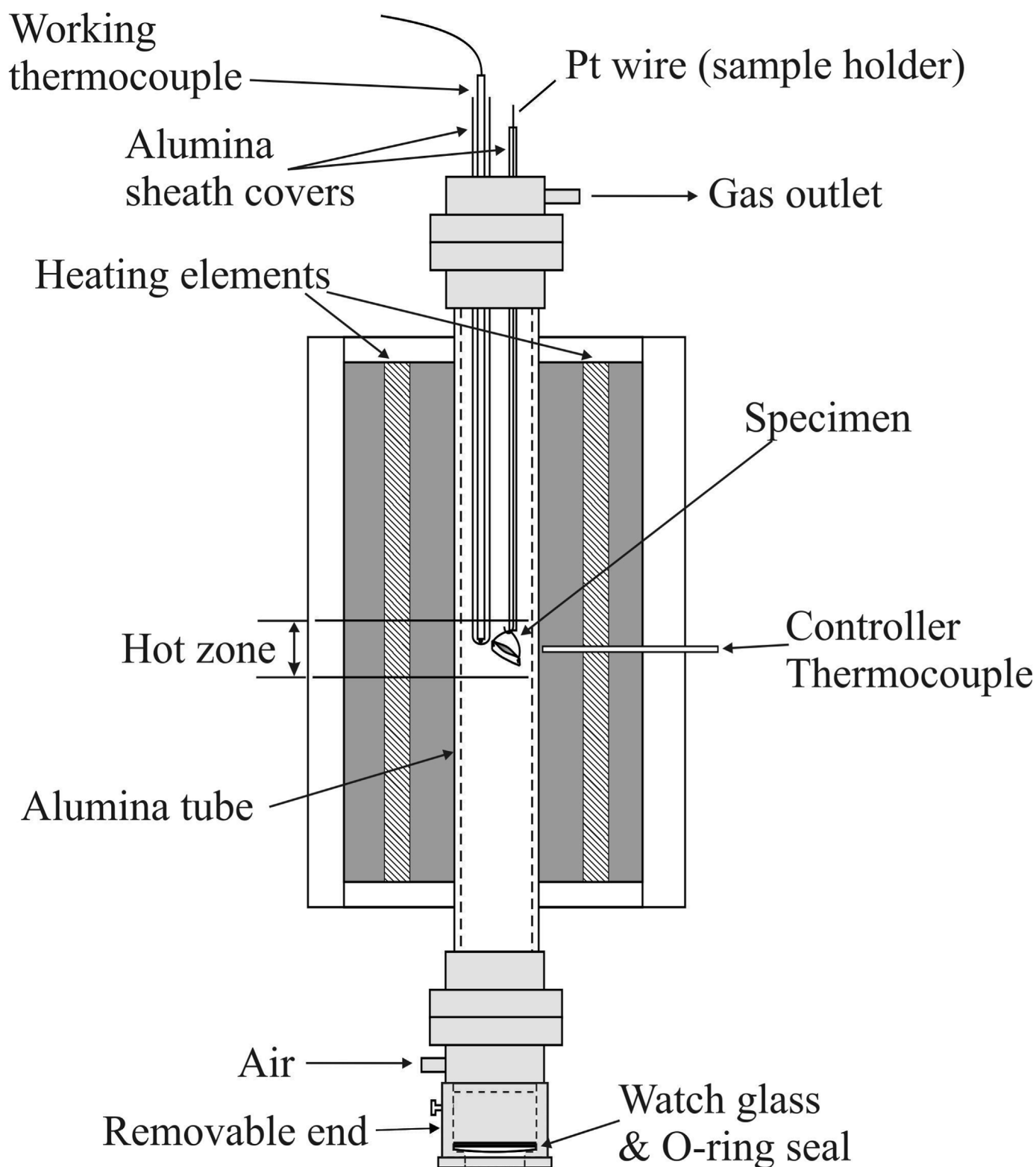


Fig. 1. Schematic diagram of (a) vertical tube furnace; (b) silica crucible; (c) platinum envelop used in the present study.

transformed into the amorphous phase. The phases presented in the samples and compositions of each phase were determined by electron probe X-Ray micro-analyzer (EPMA) [21].

Chemicals used for the present study included SiO_2 (Sigma-Aldrich, purity 99.9%, fused) and V_2O_5 (Sigma-Aldrich, purity 99.6%). These chemicals were ground and mixed thoroughly in an agate mortar for 30 min. Approximately 0.2 g of mixture was pelletized for each

experiment. The composition of the sample was selected so that both solid phase and liquid phase would be present at the target temperature.

The high-temperature experiments were conducted in a vertical tube furnace. The schematic diagram for the furnace is shown in Fig. 1 (a). The furnace is heated by the LaCrO_4 heating elements and can maintain the temperature at a constant value within ± 2 °C. A

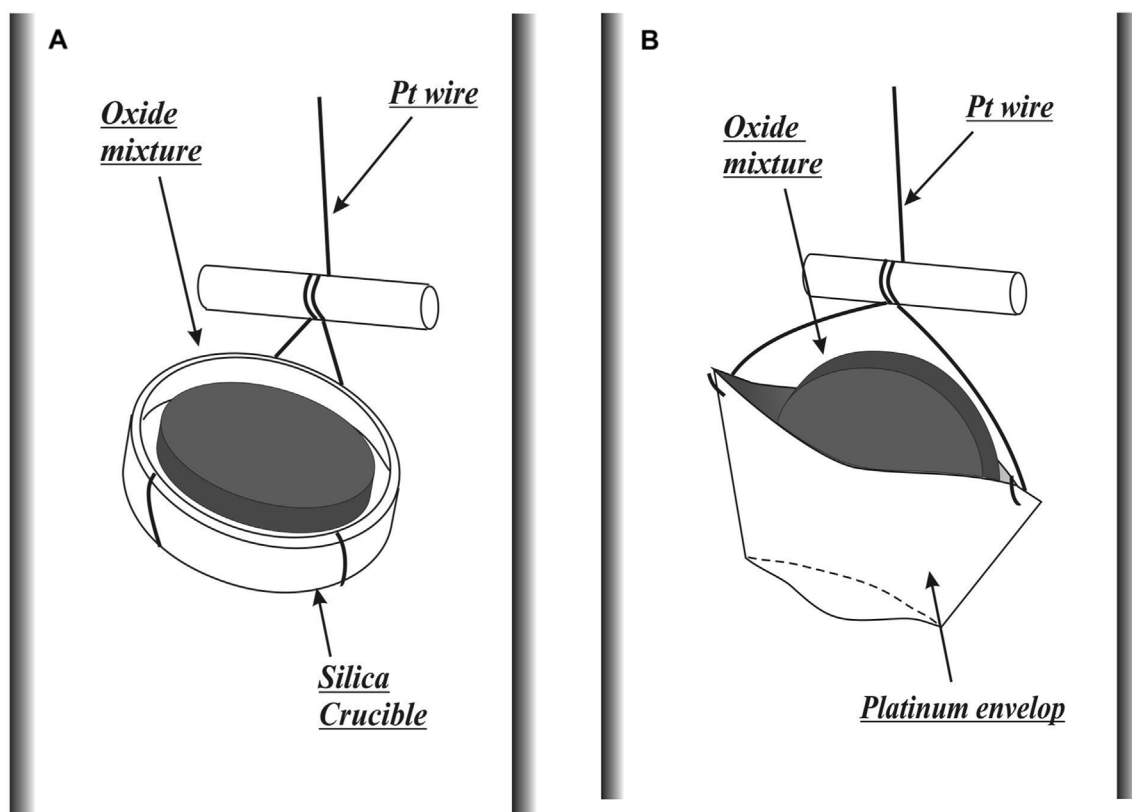


Fig. 1. (continued)

calibrated R-type thermocouple was installed to monitor the actual temperatures of samples.

Samples were held in silica crucibles (purity 99.9 wt%, Fig. 1(b)) for the experiments in equilibrium in SiO_2 primary phase or platinum envelopes (Fig. 1(c)) in V_2O_5 primary phase. Samples along with the crucibles were raised to the hot zone and suspended by Pt wire. In the present study, all the experiments were carried out in air and the air was pumped into the furnace from the bottom gas inlet as shown in Fig. 1 (a). All mixtures were preheated at 600 °C for 1 h to minimize the vaporization at temperatures higher than the melting point of V_2O_5 . After pre-treatment, temperature was increased to the target one and the sample was equilibrated at this temperature for the required period. It should be noted that only the final composition after equilibration was used for constructing the phase diagram, and the loss of V_2O_5 at high temperatures would not affect the final results.

After equilibration, samples were quenched directly into mineral oil by pulling the platinum wire and the samples were dropped freely to the quenching reagent. Negligible weight losses were detected for samples after quenching and kept in the oil for 2 days, which indicates that V_2O_5 , SiO_2 and glassy phase are non-soluble in mineral oil. Water was not chosen as the quenching reagent due to the slight solubility of V_2O_5 in water (0.7 g/L) [22]. All samples were then carefully washed by ethanol, dried and mounted in epoxy resin and polished for EPMA examinations.

The polished samples were coated with carbon using JEOL (Japan Electron Optics Ltd) Carbon Coater for electron microscopic examination. A JXA 8200 Electron Probe X-ray Micro-analyzer with Wavelength Dispersive Detectors was used for microstructure and composition analysis. The analysis was conducted at an accelerating voltage of 15 kV and a probe current of 15 nA. The standards used for analysis were from Charles M. Taylor Co. (Stanford, California): pure vanadium metal for V and CaSiO_3 for Si. The ZAF correction procedure supplied with the electron probe was applied. The average accuracy of the EPMA measurements is within 1 wt% of its elemental concentrations [23]. It

should be noted that the totals of EPMA analysis in all the measurements were close to 100 when selecting SiO_2 and V_2O_5 as the target components, which confirms that V is present as +5 valence under the present temperature ranges in air. In general, 10–20 and 5–10 measurements were performed at different areas of the sample for liquid and solid phases, respectively. The examination of compositions in the samples close and far away from the containers shows that the compositions of the samples accepted were close. Only the compositions with standard deviations less than 1 wt% were used in the construction of the phase diagram. The homogeneities of compositions in the phases indicate that the sample reached equilibrium.

3. Results and discussion

3.1. Determination of suitable equilibrium time

It is essential to ensure the samples to achieve equilibrium at high temperatures. The equilibrium conditions were examined by checking the consistency of compositions in samples held for three different periods. In the present study, three samples with an identical starting composition were held at 680 °C for 6, 16 and 48 h, respectively. The microstructures of the samples show that in all three samples, only two phases, the liquid phase and SiO_2 phase, were present. The compositional results analyzed by EPMA are listed in Table 1.

From Table 1, the results show that both SiO_2 phase and liquid phase in these three samples have close compositions. Therefore, it can be concluded that 6 h of holding time has been enough for the sample to reach equilibrium at 680 °C, which is the lowest temperature for the formation of liquid phase in this study. In the present study, to ensure that all samples reach equilibrium, they were equilibrated for 16 h.

Table 1
The compositions of the samples equilibrated for different holding time.

Temperature (°C)	Holding time (hours)	Phase	Composition (wt%)	
			SiO ₂	V ₂ O ₅
680	48	Liquid	2.0	98.0
		SiO ₂	98.8	1.2
	16	Liquid	2.0	98.0
		SiO ₂	98.9	1.1
	6	Liquid	2.1	97.9
		SiO ₂	98.8	1.2

3.2. Determination of liquidus temperatures in the SiO₂ and V₂O₅ primary phase fields

A typical microstructure of quenched sample including liquid phase in equilibrium with SiO₂ crystal is shown in Fig. 2. In Fig. 2, it could be seen that the liquid phase is spreading out without definite shape, and SiO₂ solids are shown as crystalline shapes precipitated out from the liquid phase. As the fused SiO₂ (non-crystalline) was used as one of the starting materials, the presence of newly formed SiO₂ crystals indicated that the equilibrium has been achieved and the present liquid composition was within the SiO₂ primary phase field. By fast quenching, the liquid phase was converted into the glass phase. The compositions of liquid and solid phases presented in different samples measured by EPMA are given in Table 2. EPMA analysis shows that limited SiO₂ was dissolved in the liquid phase. At the equilibrium temperature of 680 °C, the liquid phase only contains 2.0 wt% SiO₂. When the liquidus temperature increased to 900 and 1100 °C, 3.8 and 7.1 wt% SiO₂ were dissolved in the liquid, respectively. From the perspective of phase diagram, the results indicate that SiO₂ has a large primary phase field in SiO₂–V₂O₅ system starting from 2.0 wt% to 100 wt%. The studies of SiO₂ crystal compositions show that up to 1.4 wt% V₂O₅ can be dissolved in SiO₂ phase as seen in Table 2.

The determination of liquidus temperature in V₂O₅ primary phase field is practically difficult due to its extremely narrow area. Moreover, as molten V₂O₅ has high vapor pressure [20], V₂O₅ may evaporate during the experiment. Once V₂O₅ is vaporized, the bulk composition

Table 2
Experimentally determined phase compositions for the SiO₂–V₂O₅ system in the SiO₂ and V₂O₅ primary phase fields.

Sample Number	Temperature (°C)	Phase	Composition (wt%)	
			SiO ₂	V ₂ O ₅
1	680	Liquid	2.0	98.0
		SiO ₂	98.9	1.1
2	700	Liquid	2.1	97.9
		SiO ₂	98.8	1.2
3	800	Liquid	2.9	97.1
		SiO ₂	98.6	1.4
4	900	Liquid	3.8	96.2
		SiO ₂	98.6	1.4
5	1000	Liquid	5.3	96.8
		SiO ₂	98.7	1.3
6	1100	Liquid	7.1	92.8
		SiO ₂	98.7	1.3
7	680	Liquid	1.0	99.0
		V ₂ O ₅	0.1	99.9

might shift towards the SiO₂-rich direction and establish a new equilibrium, which bulk composition may enter the fully liquid zone or even the silica primary phase field. One successful experiment was obtained in the targeted V₂O₅ primary phase field. Fig. 3 shows the microstructure of sample quenched from 680 °C where the liquid phase was in equilibrium with V₂O₅ solids, which show crystalline shapes and distribute in the liquid phase. Table 2 shows that in Sample 7, the liquid phase contains 99.0 wt% V₂O₅ and balanced SiO₂ at 680 °C, and a negligible amount of SiO₂ dissolved in the V₂O₅ phase (< 0.1 wt% SiO₂ in the V₂O₅ crystal).

3.3. Determination of the eutectic temperature and composition

The eutectic temperature and composition were also determined in this study. Two experiments were conducted at 660 °C and 670 °C using Pt envelopes for 48 h to locate the eutectic temperature range and their compositions were given in Table 3. Fig. 4 gives the microstructure of Sample 9 held at 670 °C. Careful examination shows that only solid SiO₂ and V₂O₅ crystals are present in the sample and no liquid phase is

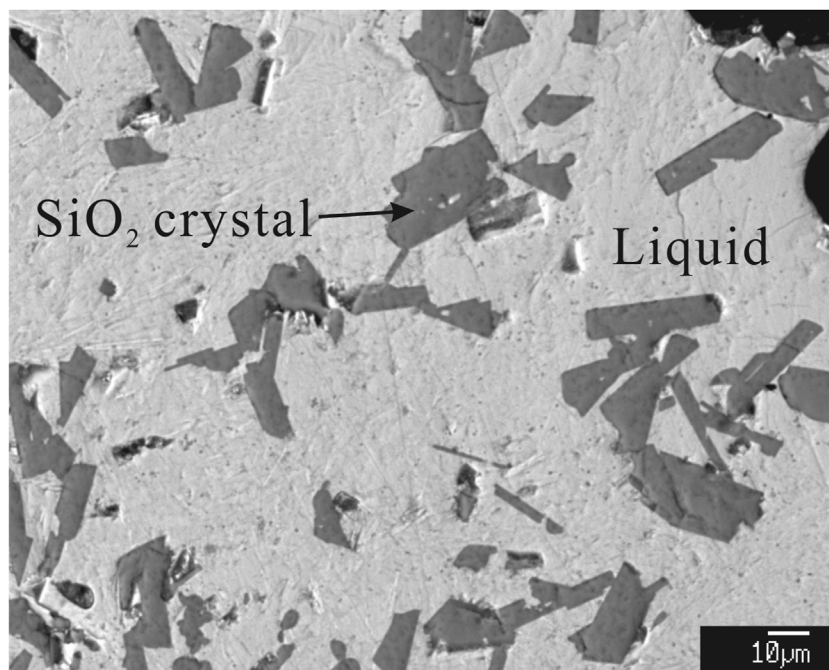


Fig. 2. The typical microstructure of liquid phase in equilibrium with SiO₂ crystal (Sample 6).

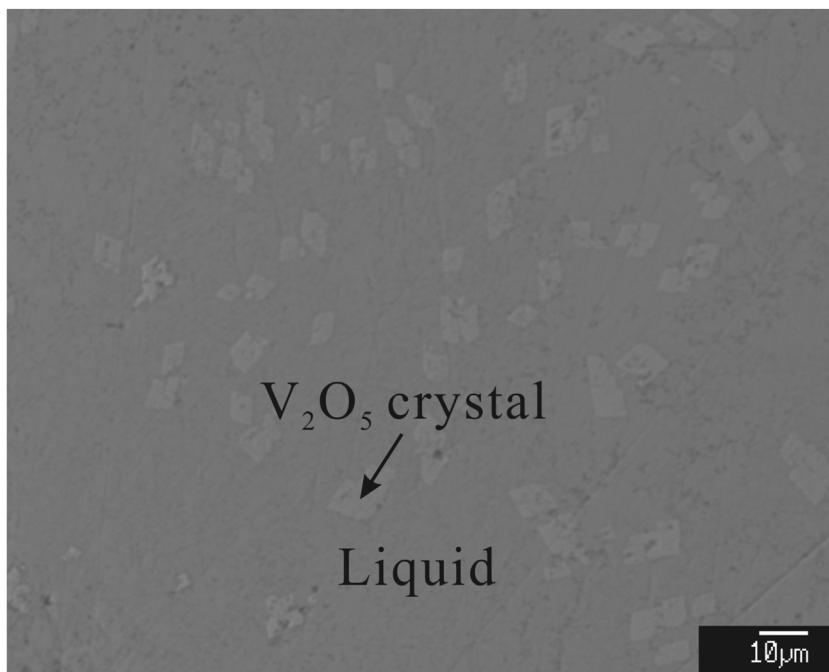


Fig. 3. The typical microstructure of liquid phase in equilibrium with V₂O₅ crystal (Sample 7).

Table 3
Experimentally determined phase compositions for the SiO₂–V₂O₅ system at 660 and 670 °C for 48 h.

Sample Number	Temperature (°C)	Phase	Composition (wt%)	
			SiO ₂	V ₂ O ₅
8	660	V ₂ O ₅	0.1	99.9
		SiO ₂	99.0	1.0
9	670	V ₂ O ₅	0.1	99.9
		SiO ₂	99.0	1.0

detected. Considering both Samples 1 and 7 at 680 °C with the liquid phases in two different primary phase field, the results indicate that the eutectic temperature in the SiO₂–V₂O₅ system should be between 670 °C and 680 °C.

In order to obtain an accurate eutectic composition, special experimental procedures were conducted. Repeated experiments with samples were firstly held at temperature 1100 °C for 16 h, followed by descending the sample to the quenching oil but not dropping freely. The starting composition, which was the same as Sample 6, was used to prepare all the samples. By this means, relatively longer cooling time was controlled and it was expected that excess V₂O₅ could start to precipitate from the liquid phase swiftly and liquid composition might

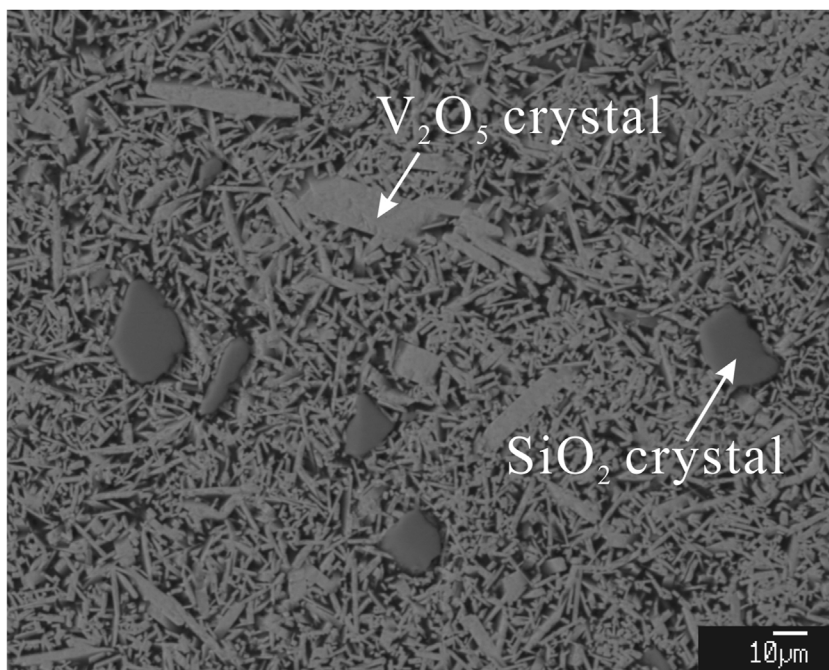


Fig. 4. The typical microstructure of V₂O₅ crystal in equilibrium with SiO₂ crystal (Sample 9).

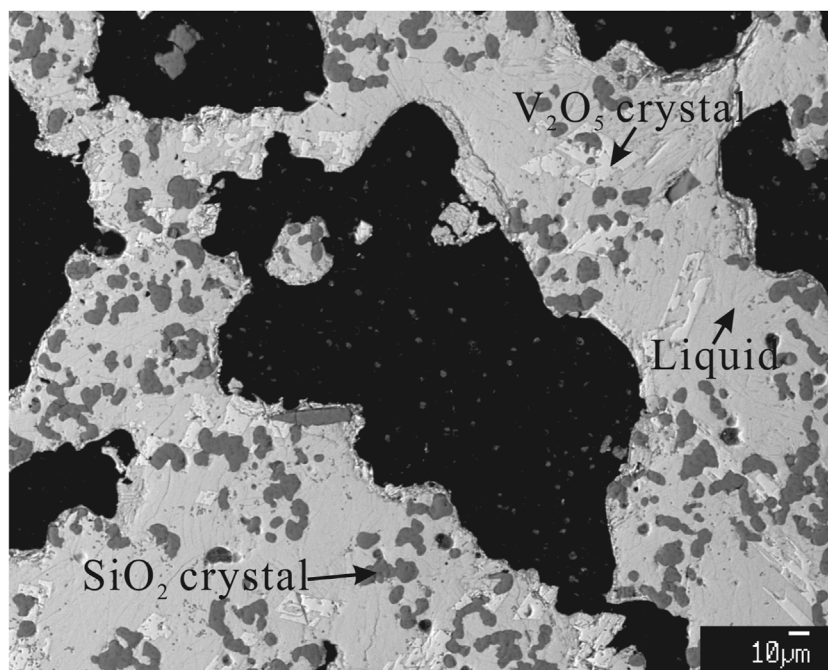


Fig. 5. The typical microstructure of slow cooled sample, liquid phase with SiO_2 crystal and V_2O_5 crystal (Sample 11).

Table 4

Experimentally determined phase compositions for the SiO_2 – V_2O_5 system to obtain the eutectic composition.

Sample Number	Cooling method	Phase	Composition (wt%)	
			SiO_2	V_2O_5
10	Slow-cooled sample	Liquid	1.9	98.1
		SiO_2	98.6	1.4
		V_2O_5	0.1	99.9
11	Slow-cooled sample	Liquid	1.9	98.1
		SiO_2	98.7	1.3
		V_2O_5	0.1	99.9

reach the eutectic composition. Two samples were obtained with the co-existences of liquid, SiO_2 and V_2O_5 crystals, as seen in Fig. 5. The EPMA results show that both of these two as-quenched samples have homogeneous liquid composition and the composition of the liquid phase are identical as shown in Table 4 (1.9 wt% SiO_2). Therefore, these two experiments demonstrate that the eutectic point is located at 1.9 wt% SiO_2 . It should be noted that due to the insufficient reaction time, the compositions of the stable SiO_2 solid solutions for Sample 10 and 11 are remaining the same as that in Sample 6 (1100 °C).

3.4. Construction of phase diagram in the SiO_2 – V_2O_5 system

Based on the present study and the melting point of pure V_2O_5 [24], the phase diagram of SiO_2 – V_2O_5 system is constructed and shown in Fig. 6. The transformation temperature of quartz and tridymite at 870 °C was adopted from the literature [25], and the SiO_2 transition is expressed by a dash line in Fig. 6.

Table 5 compares the eutectic temperature and composition obtained from this study and results from the previous studies [17,18]. The present result is close to the result reported by Gravette et al. [17]. It is noticed that Gravette et al. [17] adapted 670 °C as the melting temperature for V_2O_5 while this study applied 690 °C [24]. The melting temperature for V_2O_5 is still in dispute [24,26]. The eutectic temperature is close to the V_2O_5 melting temperature so 20 °C difference in the V_2O_5 melting temperature can cause a significant error. The results

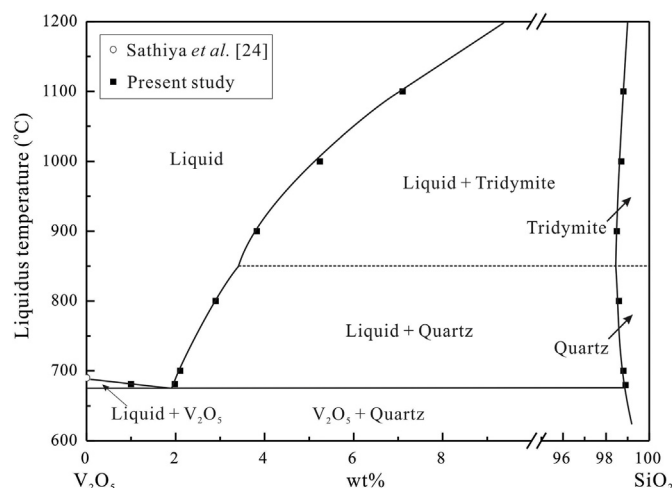


Fig. 6. The phase diagram in the SiO_2 – V_2O_5 system determined in this study.

Table 5

Comparisons of eutectic temperatures and compositions between the present study and previous results [17,18].

Sources	Eutectic Temperature (°C)	Eutectic composition (wt% SiO_2)
Gravette et al. [13]	661	1.1
Wang et al. [14]	570	32
Present study	675	1.9

from Wang et al. [18] are far from both Gravette et al.'s results and present results, which indicates their experimental methods are unsuitable.

4. Conclusions

High-temperature experiments were conducted to construct the phase diagram of SiO_2 – V_2O_5 binary system. The eutectic composition was determined to be 1.9 wt% SiO_2 and the eutectic temperature is

within 670 and 680 °C. The liquidus temperature in SiO₂ primary phase field increases rapidly with increasing SiO₂ concentration after the eutectic point. Up to 1.4 wt% V₂O₅ can be dissolved in SiO₂ to form SiO₂ solid solution. The experimental results will fill the blank in thermodynamic modelling for the V₂O₅-containing systems.

Declaration of competing interest

The authors declare that they have no known competing financial interests or personal relationships that could have appeared to influence the work reported in this paper.

Acknowledgements

The authors would like to thank Pangang Group Panzhihua Steel Research Institute Co., Ltd. (PANYAN) for financial support. The authors acknowledge the facilities, and the scientific and technical assistance, of the Australian Microscopy & Microanalysis Research Facility at the Centre for Microscopy and Microanalysis, The University of Queensland.

References

- [1] A.M. Sage, Vanadium in structural steels, *J. South Afr. Inst. Min. Metall.* 84 (5) (1984) 138–146.
- [2] P. Tian, Z. Zhong, R. Bai, X. Zhang, H. Gao, Application of different vanadium alloys in steel, CISIA Conference, 2015.
- [3] S.D. Rogers, D.W. Howie, S.E. Graves, M.J. Percy, D.R. Haynes, In vitro human monocyte response to wear particles of titanium alloy containing vanadium or niobium, *JBJS British* 79 (2) (1997) 311–315.
- [4] T. Rae, The biological response to titanium and titanium-aluminium-vanadium alloy particles: II. Long-term animal studies, *Biomaterials* 7 (1) (1986) 37–40.
- [5] G. Donald Barceloux, Vanadium, *J. Toxicol. Clin. Toxicol.* 37 (2) (1999) 265 C.
- [6] N. Bahlawane, D. Lenoble, Vanadium oxide compounds: structure, properties, and growth from the gas phase, *Chem. Vap. Depos.* 20 (7–8–9) (2014) 299–311.
- [7] Y. Yang, L. Teng, S. Seetharaman, Kinetic studies on evaporation of liquid vanadium oxide, VO_x (where x = 4 or 5), *Metall. Mater. Trans. B* 43 (6) (2012) 1684–1691.
- [8] Z. Qi, G.M. Koenig Jr., Flow battery systems with solid electroactive materials, *J. Vac. Sci. Technol.* 35 (4) (2017) 040801.
- [9] R.R. Langeslay, D.M. Kaphan, C. L. Marshall, P.C. Stair, A.P. Sattelberger, M. Delferro, Catalytic applications of vanadium: a mechanistic perspective, *Chem. Rev.* 119 (4) (2018) 2128–2191.
- [10] M.P. Vinod, D. Bahnemann, Materials for all-solid-state thin-film rechargeable lithium batteries by sol-gel processing, *J. Solid State Electrochem.* 6 (2002) 498–501.
- [11] G.N. Barbosa, H.P. Oliveira, Synthesis and characterization of V₂O₅-SiO₂ xerogel composites prepared by base catalysed sol-gel method, *J. Non-Cryst. Solids* 352 (28–29) (2006) 3009–3014.
- [12] V.N. Pak, S.V. Sukhanov, Optical properties of porous glass modified with vanadium (V) oxide, *Russ. J. Appl. Chem.* 76 (8) (2003) 1241–1244.
- [13] D.A. Kurdyukov, S.A. Grudinkin, A.V. Nashchekin, A.N. Smirnov, E.Y. Trofimova, M.A. Yagovkina, A.B. Pevtsov, V.G. Golubev, Melt synthesis and structural properties of opal-V₂O₅ and opal-VO₂ nanocomposites, *Phys. Solid State* 53 (2) (2011) 428–434.
- [14] W.A. Weyl, A.G. Pincus, A.E. Badger, Vanadium as a glass colorant, *J. Am. Ceram. Soc.* 22 (1–12) (1939) 374–377.
- [15] Y. Zhang, S. Bao, T. Liu, T. Chen, J. Huang, The technology of extracting vanadium from stone coal in China: history, current status and future prospects, *Hydrometallurgy* 109 (1–2) (2011) 116–124.
- [16] L. Wang, Y. Yao, F. Liang, Y. Dai, Y. Zhou, Z. Peng, H. Zhang, Study on Factors of Vanadium Extraction from Low-Grade Vanadium Slag with High Silicon Content by Roasting, Silicon, (2019).
- [17] N.C. Gravette, D. Barham, L.R. Barrett, An investigation of the system V₂O₅-SiO₂, *Trans. J. Br. Ceram. Soc.* (1966) 199–206.
- [18] Y. Wang, T. Guan, H. Cao, B. Xie, Z. Wei, Laboratory Research of SiO₂-V₂O₅ binary system phase diagram, *Zhongguo Xitu Xuebao* 28 (Spec) (2010) 12–15.
- [19] C.W. Bale, E. Bélisle, P. Chartrand, S.A. Decterov, G. Eriksson, A.E. Gheribi, K. Hack, I.-H. Jung, Y.-B. Kang, J. Melançon, A.D. Pelton, S. Petersen, C. Robelin, J. Sangster, P. Spencer, M.-A. Van Ende, FactSage thermochemical software and databases, 2010–2016, *Calphad* 54 (35–53) (2016).
- [20] A.J. Bergerud, Phase Stability and Transformations in Vanadium Oxide, Nanocrystals, 2016.
- [21] M. Chen, B. Zhao, J. Smialek, Phase equilibrium studies of "Cu₂O"-SiO₂-Al₂O₃ system in equilibrium with metallic copper, *J. Am. Ceram. Soc.* 96 (11) (2013) 3631–3636.
- [22] L.M. De Juan-Corpuz, R.D. Corpuz, A. Somwangthanoj, M.T. Nguyen, T. Yonezawa, J. Ma, S. Kheawhom, Binder-free centimeter-long V₂O₅ nanofibers on carbon cloth as cathode material for zinc-ion batteries, *Energies* 13 (1) (2020).
- [23] N.W. Ritchie, D.E. Newbury, S. Leigh, Breaking the 1% accuracy barrier in EPMA, *Microsc. Microanal* 18 (S2) (2012) 1006–1007.
- [24] M. Sathiy, A.S. Prakash, K. Ramesha, J.M. Tarascon, A.K. Shukla, V₂O₅-anchored carbon nanotubes for enhanced electrochemical energy storage, *J. Am. Ceram. Soc.* 133 (40) (2011) 16291–16299.
- [25] S.B. Holmquist, Conversion of quartz to tridymite, *J. Am. Ceram. Soc.* 44 (2) (1961) 82–86.
- [26] C.K. Pyo, Crystallographic and magnetic properties of V₂O₅ doped titanium cobalt ferrites, *J. Kor. Phys. Soc.* 55 (4) (2009) 1548–1552.